Modelling Pile Setup in Natural Clay Deposit Considering Soil Anisotropy, Structure and Creep Effects - A Case Study

Mohammad Rezania[a,1]; Mohaddeseh Mousavi Nezhad[b]; Hossein Zanganeh[a]; Jorge Castro[c]; and Nallathamby Sivasithamparam[d]

[a]Department of Civil Engineering, University of Nottingham, Nottingham, UK

[b]School of Engineering, University of Warwick, Coventry, UK

[c]Department of Ground Engineering and Materials Science, University of Cantabria, Santander, Spain

[d]Computational Geomechanics Division, Norwegian Geotechnical Institute, Oslo, Norway

Abstract

In this paper the behaviour of a natural soft clay deposit under installation of a case study pile is numerically investigated. The case study problem includes installation of an instrumented close-ended displacement pile in a soft marine clay, known as Bothkennar clay, in Scotland. The site was being used for a number of years as a geotechnical test bed site and the clay has been comprehensively characterised with both in-situ tests and laboratory experiments. The soft soil behaviour, both after pile installation and after subsequent consolidation, is reproduced via an advanced critical state-based constitutive model, namely S-CLAY1S, that accounts for the anisotropy of soil fabric and destructuration effects during plastic straining. Furthermore, a time-dependent extension of S-CLAY1S model, namely CREEP-S-CLAY1S is used to study soft soil creep response and the significance of its consideration on examining the overall pile installation effects. The simulation results are compared against field measurements, and for comparison the pile installation is also analysed using the Modified Cam-Clay (MCC) model to highlight the importance of considering inherent features of natural soil behaviour in the simulation. Considerable sensitivity analysis is also performed to evaluate the influence of initial anisotropy and bonding values on simulations results and to check the reliability of the numerical analyses.

[1]Corresponding author. Tel.: +44 115 95 13889.
E-mail addresses: mohammad.rezania@nottingham.ac.uk.

Introduction

Since piles have to carry design loads for long period of time, the consequences of soil modification around the pile, caused by its installation, are of great importance to variations of pile capacity. This is of more concern for piles in clays as for them the end bearing usually contributes a small part in the overall pile capacity; while skin friction along the shaft constitutes the major portion of the pile function especially when there is no reliable soil layer at the end point of the pile. Therefore, field and laboratory investigation of the effects of pile installation on the properties of natural clays has been the topic of a large number of research studies over the past few decades (e.g. Holtz and Lowitz 1965, Roy et al. 1981, O'Neill et al. 1982, Azzouz and Morrison 1988, Bond and Jardine 1991, Burns and Mayne 1999, Pestana et al. 2002, Gallagher et al. 2005). However, there are still considerable uncertainties involved in predicting the capacity and performance of frictional driven piles in clays (Niarchos 2012). Particularly the increase in the capacity of displacement piles with time in clayey deposits, that are subject to significant increase in pore pressure during pile setup, has been widely debated (e.g. Randolph et al. 1979, Kavvadas 1982, Konrad and Roy 1987, Fellenius et al. 1989, Svinkin et al. 1994, Clausen and Aas 2000, Augustesen et al. 2006, Liyanapathirana 2008, Gwizdała and Więcławski 2013). Reliable prediction of installation effects of piles on the inherent properties of natural deposits in which they are installed is essential for accurate and efficient design of these CO2 heavy and relatively expensive geo-structures. However, in most of the studies so far primarily simple analytical methods have been developed or employed to simulate changes of soil properties around the pile shaft during and after installation. This is in large part due to the lack of numerical models capable of simulating influential features of natural soil behaviour, such as anisotropy, inter-particle bonding and degradation of bonds, rate dependency and etc., at a practical scale.

The main objective of this study is to numerically analyse the effects of a single pile setup in a cohesive soil layer, by primarily evaluating the effective stress variations and pore pressure dissipations around the pile after installation and during subsequent equalisation (i.e. dissipation of excess pore pressures). It is also aimed to illustrate the practical capabilities of advanced soil models for evaluating soil alteration due to pile driving and prediction of pile capacity with time from a numerical standpoint. Pile installation is modelled with undrained expansion of a cylindrical cavity in the soil medium, commonly known as Cavity Expansion Method (CEM) (Soderberg 1962, Randolph et al. 1979, Yu 1990, Yu 2000). The numerical analyses are conducted using an anisotropic critical state-based effective stress soil model and a new time-dependent creep constitutive model. Analyses of the soil-pile load transfer mechanism or the

mechanical response in the pile structure are beyond the scope of this paper and hence are not addressed here.

Constitutive Models

It is a well-established fact that the yield curves obtained from experimental tests (with triaxial or hollow cylinder apparatuses) on undisturbed samples of natural clays are inclined due to the inherent fabric anisotropy in the clay structure (Graham et al. 1983, Dafallias 1987, Wheeler et al. 1999, Nishimura et al. 2007). Since consideration of full anisotropy in modelling soil behaviour is not practical, due to the number of parameters involved, efforts have been mainly focused on the development of models with reduced number of parameters while maintaining the capacity of the model (Kim 2004). In order to capture the effects of anisotropy on soil behaviour, a number of researcher have proposed anisotropic elasto-plastic constitutive models involving an inclined yield curve that is either fixed (Sekiguchi and Ohta 1977) or is able to rotate in order to simulate the development or erasure of anisotropy during plastic straining (Davies and Newson 1993, Whittle and Kavvadas 1994, Wheeler et al. 2003, Dafalias et al. 2006). Among the developed anisotropic models, S-CLAY1 model (Wheeler et al. 2003) has been successfully used on different applications and accepted as a pragmatic anisotropic model for soft natural clays (Karstunen et al. 2006, Yildiz 2009, Zwanenburg 2013). In this model the initial anisotropy is considered to be cross-anisotropic, which is a realistic assumption for normally consolidated clays deposited along the direction of consolidation. The model accounts for the development or erasure of anisotropy if the subsequent loading produces irrecoverable strains, resulting in a generalised plastic anisotropy. The main advantages of the S-CLAY1 model over other proposed models are i) its relatively simple model formulation, ii) its realistic K_0 prediction, and most importantly iii) the fact that model parameter values can be determined from standard laboratory tests using well-defined methodologies (Karstunen et al. 2005). The model has been later further developed to also take account of bonding and destructuration effects (Karstunen et al. 2005), and very recently, time effects (Sivasithamparam et al. 2015) as additional important features of natural soils' behaviour. In the following the basics of these two advanced extensions of S-CLAY1 model, employed in this study, are explained in further detail.

S-CLAY1S Model

S-CLAY1S (Karstunen et al. 2005) is an extension of S-CLAY1 model that, in addition to plastic anisotropy, accounts for inter-particle bonding and destructuration of bonds during plastic

straining. In three-dimensional stress space the yield surface of the S-CLAY1S model forms a sheared ellipsoid (similar to S-CLAY1) that is defined as

$$f_y = \frac{3}{2}[\{\sigma_d - p'\alpha_d\}^T\{\sigma_d - p'\alpha_d\}] - \left[M^2 - \frac{3}{2}\{\alpha_d\}^T\{\alpha_d\}\right](p'_m - p')p' = 0 \quad (1)$$

In the above equation σ_d and α_d are the deviatoric stress and the deviatoric fabric tensors respectively, M is the critical state value, p' is the mean effective stress, and p'_m is the size of the yield surface related to the soil's pre-consolidation pressure. The effect of bonding in the S-CLAY1S model is described by an intrinsic yield surface (Gens and Nova 1993) that has the same shape and inclination of the natural yield surface but with a smaller size. The size of the intrinsic yield surface is specified by parameter p'_{mi}which is related to the size $p'_m$of the natural yield surface by parameter χ as the current amount of bonding

$$p'_m = (1 + \chi)p'_{mi} \quad (2)$$

S-CLAY1S model incorporates three hardening laws. The first of these is the isotropic hardening law similar to that of Modified Cam-Clay (MCC) model (Roscoe and Burland 1968) that controls the expansion or contraction of the intrinsic yield surface as a function of the increments of plastic volumetric strains ($d\varepsilon_v^p$)

$$dp'_{mi} = \frac{vp'_{mi}}{\lambda_i - \kappa} d\varepsilon_v^p \quad (3)$$

where v is the specific volume, $\lambda_i$is the gradient of the intrinsic normal compression line in the compression plane ($\ln p' - v$ space), and κ is the slope of the swelling line in the compression plane. The second hardening law is the rotational hardening law, which describes the rotation of the yield surface with plastic straining (Wheeler et al. 2003)

$$d\alpha_d = \omega\left[\left(\frac{3\eta}{4} - \alpha_d\right)\langle d\varepsilon_v^p\rangle + \omega_d\left(\frac{\eta}{3} - \alpha_d\right)\left|d\varepsilon_d^p\right|\right] \quad (4)$$

where η is the tensorial equivalent of the stress ratio defined as $\eta = \sigma_d/p'$, $d\varepsilon_d^p$ is the increment of plastic deviatoric strain, and ω and ω_d are additional soil constants that control, respectively, the absolute rate of the rotation of the yield surface toward its current target value, and the relative effectiveness of plastic deviatoric strains and plastic volumetric strains in rotating the yield surface. The third hardening law in S-CLAY1S model is destructuration, which describes the degradation of bonding with plastic straining. The destructuration law is formulated in such a way that both plastic volumetric strains and plastic shear strains tend to decrease the value of the bonding parameter χ towards a target value of zero (Karstunen et al. 2005), it is defined as

$$d\chi = -\xi\chi\left(\left|d\varepsilon_v^p\right| + \xi_d\left|d\varepsilon_d^p\right|\right) \quad (5)$$

where ξ and ξ_d are additional soil constants. Parameter ξ controls the absolute rate of destructuration, and parameter $\xi_d$controls the relative effectiveness of plastic deviatoric strains

and plastic volumetric strains in destroying the inter-particle bonding (Koskinen et al. 2002). The elastic behaviour in the model is formulated with the same isotropic relationship as in the MCC model requiring the values of two parameters, κ and the Poisson's ratio, v' (to evaluate the value of elastic shear modulus G').

CREEP-SCLAY1S Model

The CREEP-SCLAY1(Sivasithamparam et al. 2015) is an extension of S-CLAY1 to incorporate rate-dependent response of clays. In this model the elliptical surface of the S-CLAY1 model is adopted as the Normal Consolidation Surface (NCS), i.e. the boundary between small and large irreversible (creep) strains. Furthermore, in this model creep is formulated using the concept of a constant rate of visco-plastic multiplier (Grimstad et al. 2010) as

$$\dot{\Lambda} = \frac{\mu^*}{\tau}\left(\frac{p'_{eq}}{p'_p}\right)^{\beta}\left(\frac{M^2-\alpha^2_{K_0^{nc}}}{M^2-\eta^2_{K_0^{nc}}}\right) \tag{6}$$

where p'_p is the size of the outer rotated ellipse (see Fig. 1) which defines the NCS; p'_{eq} is the size of the inner ellipse passing through the current state of effective stress that is called the Current Stress Surface (CSS); μ^* is the modified creep index, τ is called the reference time and is set to 1 day if the NCS is derived from a standard oedometer test (see Leoni et al. 2008 for details); $\alpha_{K_0^{nc}}$ defines the inclinations of the ellipses in normally consolidated state (assuming K_0 consolidation history); $\eta^2_{K_0^{nc}} = 3(1-K_0^{nc})/(1+2\,K_0^{nc})$, and the additional term $(M^2-\alpha^2_{K_0^{nc}})/(M^2-\eta^2_{K_0^{nc}})$ is added to ensure that under oedometeric conditions, the resulting creep strain corresponds to the measured volumetric creep strain rate. Moreover, β is defined as $\beta = (\lambda^*-\kappa^*)/\mu^*$ where λ^* and κ^* are the modified compression and modified swelling indices, respectively, and μ^* is related to the one-dimensional secondary compression index, C_α, as $\mu^* = C_\alpha/[\ln 10\,(1+e_0)]$.

The size of NCS evolves with volumetric creep strains ε_v^c according to the following isotropic hardening law

$$p'_p = p'_{p0}exp\left(\frac{\varepsilon_v^c}{\lambda^*-\kappa^*}\right) \tag{7}$$

where p'_{p0} is the initial effective preconsolidation pressure. Adopting the same function as that of the NCS, the size of the CSS is obtained from the current stress state (p' and q) using the intersection of the vertical tangent to the ellipse with the p' axis as

$$p'_{eq} = p' + \frac{3}{2}\frac{\lfloor\{\sigma_d - p'\alpha_d\}^T\{\sigma_d - p'\alpha_d\}\rfloor}{\left[M^2 - \frac{3}{2}\{\alpha_d\}^T\{\alpha_d\}\right]p'} \quad (8)$$

where p'_{eq} is also known as the equivalent mean stress. The CREEP-SCLAY1 model incorporates the same rotational hardening law as that of the S-CLAY1/S-CLAY1S models. Recently, the CREEP-SCLAY1 model has been further extended (Gras et al. 2016) to take into account the soil structure by adopting the destructuration hardening law of the S-CLAY1S model, as described in the previous section. The new extended model is called CREEP-S-CLAY1S.

Case Study

Bothkennar clay is a normally consolidated marine clay deposited on the southern bank of Forth River Estuary near Stirling, located approximately midway between Glasgow and Edinburgh in Scotland. Bothkennar was the EPSRC geotechnical test site for which a comprehensive series of tests over the properties of the high plasticity silty clay at that site was performed in early 90th and reported in the collection of papers in *Géotechnique Symposium-in-Print* (Vol. 42, No. 2, 1992). Since then it has also been the subject of a number of more advanced experimental investigations (e.g. Albert et al. 2003, Houlsby et al. 2005, McGinty 2006). Lehane and Jardine (1994) conducted a series of field experiments using high quality instrumented piles developed at Imperial College. The displacement piles employed in the investigation were equipped to measure pore pressures and effective stresses acting on the soil-pile interface during pile installation and following consolidation. Two different pile lengths of 3.2m and 6m were studied, and the diameter of the case study piles was uniformly 102mm. The cone-ended steel tubular piles were jacked into the ground from the base of a 1.2m deep cased hole. The general configuration of the 6m long model pile is shown in Fig. 2.

As shown in the figure different sensors to measure axial load, radial stress, shear stress and pore pressure were used at three clusters located along the lower 3m section of the pile, further details with regards to instrumentations can be found in Bond et al. (1991). The profile of the natural deposit penetrated by the instrumented piles can also be seen in Fig. 3, it includes a 1m deep over-consolidated dry crust followed by 5m of lightly overconsolidated Bothkennar clay with Over Consolidation Ratio (OCR) value of around 1.5.

Numerical Model and Simulations

The two advanced constitutive models described in above have been implemented as user defined models in PLAXIS 2D AE version (Brinkgreve et al. 2013) using the fully implicit numerical solution proposed by Sivasithamparam (2012). Using each of the implemented advanced models for the deformation, PLAXIS carries out the coupled flow-deformation consolidation analysis based on Biot's theory.

The geometry of the numerical model for pile installation and the schematic sketch of different soil layers are shown in Fig. 4. As it is shown in the figure the groundwater table is located 1m below the ground surface. Taking advantage of the symmetry of the problem, axisymmetry condition is assumed in the finite element analysis. Parametric studies were carried out to find out how wide the model should be to have a negligible influence of the outer boundary. An extent of 3m from the symmetry axis in the horizontal direction was found to be sufficient. The depth of the model was selected to be the same as the length of the pile (i.e. 6m) in order to avoid modelling the pile tip, which can cause numerical instabilities. Roller boundaries are applied to all sides in order to enable the soil moving freely due to cavity expansion. Drained conditions and zero initial pore pressures are assumed above the water table. Also a drainage boundary is considered at the ground level and dynamic effects are ignored in the numerical model. A finite element mesh with 4048 15-noded triangular elements, resulting in 33021 nodes, is used in the analyses, with extra degrees of freedom for excess pore pressures at corner nodes (during consolidation analysis). Mesh sensitivity studies were done to ensure that the mesh is dense enough to produce accurate results for both of the constitutive models. Towards the cavity wall much finer elements are used in order to provide better resolution in this zone with expected high strain gradients. The problem is modelled using large strain analyses with updated pore pressures, taking advantage of PLAXIS's updated Lagrangian formulation.

Undrained pile installation is modelled as the expansion of a cylindrical cavity through development of a prescribed displacement from a small initial radius to a final, larger, radius (see Fig. 4). There are other techniques for modelling the expansion of the cavity, e.g. applying an internal volumetric strain, however a prescribed displacement is proven to be more practical particularly in terms of numerical stability (for further details see Castro and Karstunen 2010). As stated above, there is extensive laboratory data available for Bothkennar clay which makes it possible to derive a consistent set of material parameters for the advanced constitutive models being used for the soft soil layer in this study. The initial values of state variables, as well as the values of conventional soil constants and additional soil parameters used in the models are

summarised in Table 1. The initial state variables include the initial void ratio e_0, overconsolidation ratio *OCR*, as well as the initial amount of anisotropy α_0 and bonding χ_0 (see Table 1). The conventional soil constants include the unit weight γ, the elastic constants (slope of the swelling line κ and Poisson's ratio v'), and the plastic constants (slope of the normal compression line λ and the critical state line M, respectively). Based on the λ and κ values, and the initial void ratio, it is easy to calculate the corresponding values for the CREEP-S-CLAY1S model (λ^*=0.10 and κ^*=0.0067). In Table 1, the additional soil constants related to the evolution of anisotropy (ω and ω_d) and destructuration (ξ and ξ_d), are also listed together with the intrinsic compressibility λ_i. The latter needs to be used as input instead of λ for a natural soil, when a model with destructuration is used. The methodology for deriving these soil constants has been discussed e.g. by Leoni et al. (2008) and Sivasithamparam et al. (2015) and is not repeated here.

Table 1. Model parameter values for Bothkennar clay.

Basic parameters								Anisotropy			Bonding			
$\gamma\ (kN/m^3)$	e_0	OCR	K_0	κ	v'	λ	M	α_0	ω	ω_d	χ_0	λ_i	ξ	ξ_d
16.5	2	1.5	0.5	0.02	0.2	0.3	1.5	0.59	50	1	8	0.18	9	0.2

Table 2 lists the values for the viscosity parameters which are similar to the Soft Soil Creep (SSC) model (Vermeer et al. 1998), and the Anisotropic Creep model (ACM) (Leoni et al. 2008).

Table 2. Additional creep parameter values for Bothkennar clay.

μ^*	μ_i^*	τ (days)
2×10^{-3}	5.07×10^{-3}	1

During the consolidation coupled analysis, the permeability coefficient k is assumed to be constant. The values for soil permeability (summarised in Table 3) were obtained from conventional oedometer tests, horizontal permeability k_h from tests on horizontal samples and vertical permeability k_v from tests on vertical samples (Géotechnique Symposium-in-Print 1992).

Table 3. Permeability values for Bothkennar clay deposit.

Depth (m)	k_h(m/day)	k_v(m/day)
0-1	2.42×10^{-4}	1.21×10^{-4}
1-6	1.21×10^{-4}	5.96×10^{-5}

The behaviour of the over-consolidated dry crust layer was modelled with a simple linear elastic-perfectly plastic Mohr-Coulomb model using the following relevant parameter values for the Bothkennar clay: E =3 MPa, v'=0.2, φ'=30°, ψ'=0°, c'=6 kPa, and γ =19 kN/m^3. It should also be added that the initial state of stress was generated by adopting K_0-procedure (Brinkgreve et al. 2013). In addition to the two advanced models, S-CLAY1S and CREEP-S-CLAY1S, the boundary value problem was also modelled with the commonly used MCC model in order to better highlight the advantages of considering natural features of soil behaviour in the simulation.

Numerical Simulations Results

Total stress, pore pressure and effective stress variations

Experimental measurements and numerical predictions of radial total stresses at the pile surface are shown in Fig. 5. This figure illustrates that similar to the experimental results, the S-CLAY1S and CREEP-S-CLAY1S models predict the radial stresses to lie between the initial undisturbed horizontal stress, σ_{h0}, and the pressuremeter limit pressure. The figure also shows that the MCC model overestimates the radial total stresses and predicts them to exceed the pressuremeter limit pressure at depths beyond 3.5m.

The numerical predictions of Fig. 5, which are qualitatively consistent with the experimental results, indicate that the radial total stresses in Bothkennar clay increase with the increase of penetration depth. Such trend has also been observed in similar studies on other types of clay (Doherty and Gavin 2011; Randolph 2003) which suggest that the increase of total radial stresses with depth intensifies with the preconsolidation pressure of clay layers. Moreover, a comparison between Figs. 3(b) and 5 shows that the variations of σ_{ri} resembles the end resistance variations with depth which infers that σ_{ri} is controlled by the soil state (Doherty and Gavin 2011) contrary to sandy soils in which variations of σ_{ri} is independent of the soil state (Chow and Jardine 1996).

For a proper understanding of pile behaviour and to draw a clearer picture of effective stress conditions, pore pressure values should be provided in addition to radial total stresses. Fig. 6 shows the experimentally measured pore pressures and their corresponding numerical predictions obtained through MCC, S-CLAY1 and CREEP-S-CLAY1S models. The figure illustrates that the numerical results fit well within the experimental measurements and predict similar trends. The predictions made via MCC and S-CLAY1S models are approximately equal

while the CREEP-S-CLAY1S model predicts slightly higher pore pressure values. Nevertheless all three models predict a linear increase in pore pressure as depth increases. Such overall trend can be seen in the experimental results as well, except that in the experimental results, depending on penetration depth, two different manners can be distinguished. In other words, as it is indicated by Doherty and Gavin (2011), for penetration depths less than 2.5m, pore pressure increases rapidly and after this depth its rate reduces. Similar trend was observed in Fig. 5 for radial total stresses as well. This similar tendency could be attributed to friction fatigue (Xu et al. 2006) and as it can be seen in Figs. 5 and 6 the numerical results of SCLAY1S and CREEP-S-CLAY1S can capture this feature and predict similar tendency for σ_{ri} and pore pressure.

Pore pressure equalisation and radial total stress relaxation are two of the main features of the Imperial College pile tests (Doherty and Gavin 2011). These features are quantified through normalised parameters of pore pressure dissipation factor U_d and relaxation coefficient H/H_i which are defined as:

$$U_d = \frac{u_{max} - u}{u_{max} - u_0} \tag{9}$$

$$\frac{H}{H_i} = \frac{\sigma_r - u_0}{\sigma_{ri} - u_0} \tag{10}$$

where u is the pore pressure after installation and subsequent consolidation, u_0 the hydrostatic (ambient) water pressure, u_{max} maximum pore pressure attained during pile installation and σ_r the radial total stress during consolidation. Experimental measurements of these two factors are depicted in Figs. 7(a) and (b) and are compared with their numerical counterparts predicted via MCC, S-CLAY1S and CREEP-S-CLAY1S models. The trends predicted with these models for reduction of pore pressure during consolidation match well with the experimental data (Fig. 7(a)).

The MCC and CREEP-S-CLAY1S models provide comparably similar estimations of pore pressure equalisation factors which are smaller than S-CLAY1S predictions. As it was discussed earlier in the paper, variations of radial total stress mirror the pore-pressure changes; hence the trend of H/H_i experimental results is similar to U_d. Such behaviour has been reasonably predicted with S-CLAY1S and CREEP-S-CLAY1S models while MCC can only predict such qualitative behaviours for the early stages of pile consolidation, and it overestimates pile relaxation factor after half a day of consolidation (i.e. after 700 minutes).

Because total radial stress does not decrease as much as pore pressures during consolidation, the radial effective stress increases towards a final equilibrium radial effective stress σ'_{rc}. Fig 7(c) shows the comparison between experimental and numerical variations of

normalised radial effective stress σ_r'/σ_{rc}' during equalisation. As it can be seen in this figure, all three models can capture increasing trend of σ_r'/σ_{rc}' and their quantitative consistency with experimental results reduces from S-CLAY1S to CREEP-S-CLAY1S and MCC models. Numerical predictions of variations of equalised radial effective stress with depth are depicted in Fig. 8 and are compared with experimental results. As this figure illustrates, all models predict σ_r' to increase with depth, however the most quantitatively comparable results to field measurements are provided by CREEP-S-CLAY1S model. As it was indicated by Randolph (2003), the reliability of existing predictive models for accurate evaluation of effective stresses is one of the main concerns regarding application of these models. The comparisons carried out in this section show that CREEP-S-CLAY1S model provides more accurate and reliable results compared to the other two time-independent models.

Variations of Undrained shear Strength

Figs. 9(a) and (b) show the variation of normalised undrained shear strength c_u/c_{u0} (where c_u is the undrained shear strength and c_{u0} is the undrained shear strength of undisturbed soil) in the vicinity of the pile, predicted via MCC, S-CLAY1S and CREEP-S-CLAY1S models, both after column installation and after consolidation. Experimental studies show that installing displacement piles in soft soils results in reduction of undrained shear strength of the soil right after pile installation (Serridge and Sarsby 2008). Fig. 9(a) illustrates that while S-CLAY1S and CREEP-S-CLAY1S predict this reduction, MCC model fails to capture such reduction. The results depicted in Fig. 9(a) also suggest that big reductions occur for soils in close vicinity of the column (less than 3 column radii) and beyond that there is a slight decrease in undrained shear strength. As it is discussed by Castro and Karstunen (2010), the large reductions of undrained shear strength can be attributed to the loss of apparent bonding and small reductions are owing to the reduction of effective mean pressure.

After consolidation, the undrained shear strength increases (Fig. 9(b)). This increase in close vicinity of the pile is more severe and in further distances from the column in areas which are less affected by the pile, this increase is minimal. However, the estimations of this increase, provided by the three constitutive models, are different. For instance, close to the cavity wall, MCC model provides predictions which can be up to 90% different from S-CLAY1S and CREEP-S-CLAY1S models, while beyond fifteen pile radii all three models are quantitatively similar. Fig. 10 shows the variations of undrained shear strength near the cavity wall and during the equalisation period. As it can be seen in this figure, S-CLAY1S and CREEP-S-CLAY1S

models predict that the undrained shear strength, right after column installation, are 50% and 30% less than c_{u0}, while MCC predicts it to be 40% more than c_{u0}. As time elapses and excess pore pressure dissipates, all three models show increasing undrained shear strength due to excess pore pressure dissipation and increase in mean effective stresses. The CREEP-S-CLAY1S model, in the early stages of consolidation predicts higher undrained shear strength than the S-CLAY1S model; however its equalised undrained shear strength is smaller because creep causes relaxation of radial stresses.

Sensitivity Analysis

Penetration of a pile in a natural soft clay deposit results in destructuration, i.e. degradation of the soil internal structure, which consequently influences the yielding of the soil. In this section the sensitivity of numerical predictions of soil behaviour during equalisation is investigated against variations of initial anisotropy and bonding (represented by parameters α_0 and χ_0 respectively) which indicate the state of the yield surface inclination and structure of the soil at the onset of the consolidation stage. Fig. 11 shows the S-CLAY1S and CREEP-S-CLAY1S predictions of radial effective stresses for α_0 values changing ±20% around its representative value. This figure illustrates that the higher the initial anisotropy parameter is, the lower the predicted radial effective stress would be. However, comparing these results with corresponding results in Fig. 8 shows that using α_0 with ±20% different values does not have a significant qualitative and quantitative effect on numerical results. Similar trends can be distinguished in Fig. 12 which depicts the effect of χ_0 variations on numerical predictions of radial effective stresses.

The sensitivity of numerical results, in time domain, to the alteration of initial bonding and anisotropy parameters is shown in Figs. 13 and 14, respectively. As these two figures show, ±20% variation of these parameters does not have considerable effect on numerical predictions. Overall, the sensitivity analyses performed in this section confirms that initial value of anisotropy and bonding parameters has negligible effects on numerical predictions of S-CLAY1S and CREEP-S-CLAY1S models, and therefore for a reasonably accurate evaluation of the initial values of anisotropy and bonding, these models performance are reliable.

Installation effect on soil structure

The effect of pile setup on surrounding soil structure can be investigated through the variations of bonding parameter χ which represents the sensitivity of the soil. Fig. 15 shows the S-CLAY1S and CREEP-S-CLAY1S predictions of normalised bonding parameter, in different

distances from pile surface, after column installation and soil consolidation phases. The results illustrated in this figure are obtained for different initial bonding parameter values to confirm that χ_0 has no major effect on numerical simulation results and hence can be reasonably utilised for normalisation of χ. Fig. 15 illustrates that installation of pile results in the reduction of bonding parameter. This reduction is understandably more intense close to the pile surface. Moreover, the figure also shows that the predictions of both S-CLAY1S and CREEP-S-CLAY1S models are comparably similar after installation. However, as time elapses and the soil consolidates, the results of rate-dependant model deviates from the rate-independent S-CLAY1S model. The comparison between χ/χ_0 after installation and after consolidation reveals that there is further reduction of bonding parameter after consolidation. This extra reduction predicted by S-CLAY1S model is smaller than that of CREEP-S-CLAY1S model. Therefore, the CREEP-S-CLAY1S model predicts the contribution of consolidation process in reduction of χ to be bigger than what it was thought before (discussed in Castro and Karstunen 2010); however it can yet be concluded that the reduction of χ is mainly caused by undrained expansion of cavity.

Installation effect on soil anisotropy

Similar to χ, installation of a pile affects the soil fabric orientation and consequently the inclination of the representative yield surface. Fig. 16 shows the variation of α for different α_0 values after installation of the column and after consolidation of the soil which are predicted via S-CLAY1S and CREEP-S-CLAY1S models. As it can be seen in this figure, after installation and consolidation, the value of anisotropy parameter in close vicinity of the column (distances up to 2 radii from the column surface) is independent of α_0 and both models provide similar predictions of α. In further distances, up to 4 column radii, while both models provide similar evaluations of α after installation, the CREEP-S-CLAY1S model predicts lower anisotropy parameter after consolidation. In distances beyond 4 column radii, the value of α depends on α_0, however the trends of numerical predictive models follow the aforementioned trends. In other words, in this radial distances from the pile both models have comparably similar evaluations of α after installation while S-CLAY1S model predicts higher α values after consolidation. Fig. 16 illustrates that, after installation, the value of α on the column surface increases when α_0=0.47 and decreases when α_0=0.59 and 0.71. After consolidation, for α_0=0.47 and 0.59, the anisotropy parameter on the column surface exceeds α_0 while remains smaller than α_0 when α_0=0.71. These trends are sustained in distances less than $1.5r_c$, and beyond that α is less than α_0 and tends toward α_0 at further distances from the column.

To clarify the trends observed in Fig. 16, variations of radial α_r and axial α_y components of anisotropy tensor are depicted in Figs. 17-20. Also to check the sensitivity of these components to the value of initial anisotropy parameter, the variations of α_r and α_y are evaluated for ±20% alteration of α_0 around its representative value and the results are depicted in Figs. 17 and 18. Similar sensitivity analysis is also carried out for the effects of alteration of χ_0 on the variations of α_r and α_y (Figs. 19 and 20). Figs. 17 and 19 suggest that α_r after installation and consolidation reduces as the distance from the surface of the pile increases; and, on the pile surface, α_r after consolidation is higher than that caused by undrained expansion of cavity. In contrary to this trend, Figs. 18 and 20 show that α_y increases as the distance increases from the pile surface. These figures also illustrate that both numerical models provide reasonably comparable results and these results are not sensitive to α_0 and χ_0 values.

Discussion

The comparison of the numerical results in two stages of pile setup history, installations and equalisation, reveals that the models which take into account the natural features of the soil behaviour, namely anisotropy, destructuration and time effects, provide comparable results during installation period (Figs. 5 and 6). The predictions of SCLAY1S and CREEP-SCLAY1S models after installation are in good agreement with the experimental measurements while the MCC model provides less comparable results. In other words, after installation, both SCLAY1S and CREEP-SCLAY1S models provide representative and approximately similar predictions of radial effective stresses, pore pressures, and undrained shear strengths (Figs. 5, 6 and 9, respectively). While MCC predictions in some cases (e.g., pore water pressure) are consistent with the two other models, in other cases its simulation results deviate from the measurement data as well as the predictions of the two advanced models. This is mainly due to the fact that pile installation significantly influences the fabric orientation and structure of the surrounding natural soils (Figs. 15 and 16), as well as their yielding characteristics, and these are the aspects of the natural soil behaviour that are not taken into account in the MCC model.

Despite undrained expansion of cavity, considerable differences can be distinguished between numerical predictions of SCLAY1S and CREEP-SCLAY1S models during equalisation period (Figs. 17-20). This is predictable as the influence of creep increases as time goes on. However, similar comparative studies by Sivasithamparam et al. (2015) showed that even during undrained loading stage, consideration of time-dependency has significant effects on the numerical simulation results, and hence it should be taken into account (particularly in case of

modelling soft and sensitive clay response). The effects that pile setup has on the variations of soil anisotropy and natural structure, both after installation and consolidation periods, are well-pronounced in Figs. 17-20. From a qualitative standpoint, both models provide predictions which are consistent with the experimental results. For instance, the experimental measurements indicate that there is a relaxation in total stresses during consolidation that leads to final radial effective stresses that are less than initial radial total stresses (Randolph 2003). Both models provide qualitatively similar results while it is the creep model that predicts more quantitatively consistent representation of the field measurements (see Figs. 5 and 7).

One of the main advantages of the recently developed CREEP-SCLAY1S model is that, unlike the majority of visoplastic models that are based on Perzina's overstress theory (Hinchberger and Rowe 2005; karstunen and Yin 2010), its viscous (creep) parameters have clear physical meaning and are relatively simple to determine. As indicated earlier in the paper, the additional parameters that S-CLAY1 family of models have, when compared to the MCC, are physically plausible parameters with established procedures for their determination that are well-explained in the literature. This simplicity of parameter determination, and the fact that these advanced models are hierarchical extensions of the widely used MCC model, makes their practical application reasonably straightforward.

Conclusions

In the present paper, alteration of a soft clayey soil due to installation of close-ended pile has been numerically investigated. For this purpose, two advanced constitutive models of S-CLAY1 family, which account for soil anisotropy, destructuration and time effects (in case of the creep model) have been used. Using fully integrated implicit numerical scheme, these model have been implemented as user-defined models in Plaxis 2D and were employed to investigate the soft soil response to pile setup. The advanced constitutive models provided reliable predictions of soil behaviour, variations of pile capacity and soil's structural alteration with time. To highlight the significance of considering natural features of soil behaviour in the modelling, corresponding numerical predictions of MCC model have also been provided. The comparison between the predictions of the time-dependent model against field measurements of the case study pile validated the capability of the CREEP-S-CLAY1S model in qualitatively and quantitatively capturing the observed soil behaviour. These comparisons also illustrated the shortcomings of classical MCC model and supported the impact of considering soil natural features for a reasonably accurate and reliable numerical modelling work. The series of sensitivity analyses that

has been carried out showed that the variations of initial values of yield surface inclination and bonding parameters have negligible effects on numerical predictions. Furthermore, these analyses showed that, while time-independent and time-dependent S-CLAY1-based models provide reasonably comparable results of the soil behaviour after pile setup, consideration of time effects better represent the changes in radial effective stresses (known as the underlying mechanism of pile installation effects for driven piles in soft clays) that occur during installation and subsequent dissipation of excess pore pressures.

References

Albert, C., Zdravkovic, L., and Jardine, R. "Behaviour of Bothkennar clay under rotation of principal stresses." *Proc., International Workshop on Geotechnics of Soft Soils-Theory and Practice. Essen Verlug Gluckauf*, 441-447.

Augustesen, A., Andersen, L., and Sørensen, C. S. (2006). "Assessment of time functions for piles driven in clay." *DCE Technical Memorandum*, Department of Civil Engineering, Aalborg University.

Azzouz, A., and Morrison, M. (1988). "Field measurements on model pile in two clay deposits." *Journal of Geotechnical Engineering*, 114(1), 104-121.

Bond, A. J., Dalton, J., and Jardine, R. J. (1991). "Design and performance of the Imperial College instrumented pile." *ASTM Geotechnical Testing Journal*, 14(4), 413-424.

Bond, A. J., and Jardine, R. J. (1991). "Effects of installing displacement piles in a high OCR clay." *Géotechnique*, 41(3), 341-363.

Brinkgreve, R. B. J., Swolfs, W. M., and Engin, E. (2013). "PLAXIS 2D anniversary edition reference manual." Delft University of Technology and PLAXIS, The Netherlands.

Burns, S., and Mayne, P. (1999). "Pore pressure dissipation behavior surrounding driven piles and cone penetrometers." *Transportation Research Record: Journal of the Transportation Research Board*, 1675, 17-23.

Castro, J., and Karstunen, M. (2010). "Numerical simulations of stone column installation." *Canadian Geotechnical Journal*, 47(10), 1127-1138.

Chow, F., and Jardine, R. J. (1996). "Investigations into the behaviour of displacement piles for offshore foundations." *International Journal of Rock Mechanics and Mining Sciences and Geomechanics Abstracts*, 33(7), 319A-320A.

Clausen, C. J. F., and Aas, P. M. (2000). "Bearing capacity of driven piles in clays." *NGI report* Norwegian Geotechnical Institute.

Dafalias, Y. F., Manzari, M. T., and Papadimitriou, A. G. (2006). "SANICLAY: simple anisotropic clay plasticity model." *International Journal for Numerical and Analytical Methods in Geomechanics*, 30(12), 1231-1257.

Dafallias, Y. "An anisotropic critical state clay plasticity model." *Proc., Proceeding of the constitive laws for engineering materials theory and applications*, 513-521.

Davies, M., and Newson, T. "A critical state constitutive model for anisotropic soil." *Proc., Predictive soil mechanics* Thomas Telford, London, 219–229.

Doherty, P., and Gavin, K. (2011). "The shaft capacity of displacement piles in clay: A state of the art review." *Geotechnical and Geological Engineering*, 29(4), 389-410.

Doherty, P., and Gavin, K. (2011). "Shaft capacity of open-ended piles in clay." *Journal of Geotechnical and Geoenvironmental Engineering*, 137(11), 1090-1102.

Fellenius, B., Riker, R., O'Brien, A., and Tracy, G. (1989). "Dynamic and static testing in soil exhibiting set-up." *Journal of Geotechnical Engineering*, 115(7), 984-1001.

Gallagher, D., Gavin, K., McCabe, B., and Lehane, B. "Experimental investigation of the response of a driven pile in soft silt." *Proc., Proceedings of the 18 th Australasian Conference on the Mechanics of Structures and Materials*, Taylor and Francis, 991-996.

Gens, A., and Nova, R. (1993). "Conceptual bases for a constitutive model for bonded soils and weak rocks." *Geotechnical engineering of hard soils-soft rocks*, 1(1), 485-494.

Graham, J., Noonan, M. L., and Lew, K. V. (1983). "Yield states and stress–strain relationships in a natural plastic clay." *Canadian Geotechnical Journal*, 20(3), 502-516.

Gras, J.-P., Sivasithamparam, N., Karstunen, M., and Dijkstra, J. (2016). "Bounding anisotropy and structure model parameters for natural fine grained materials." *Acta Geotechnica (under review)*.

Grimstad, G., Degago, S., Nordal, S., and Karstunen, M. (2010). "Modeling creep and rate effects in structured anisotropic soft clays." *Acta Geotech.*, 5(1), 69-81.

Gwizdała, K., and Więcławski, P. (2013). "Influence of time on the bearing capacity of precast piles." *Studia Geotechnica et Mechanica*, 35(4), 65-74.

Hinchberger, S. D., and Rowe, R. K. (2005). "Evaluation of the predictive ability of two elastic-viscoplastic constitutive models." *Canadian Geotechnical Journal*, 42(6), 1675-1694.

Holtz, W. G., and Lowitz, C. A. (1965). "Effects of driving displacement piles in lean clay." *Journal of the Soil Mechanics and Foundations Division*, 91(5), 1-14.

Houlsby, G. T., Kelly, R. B., Huxtable, J., and Byrne, B. W. (2005). "Field trials of suction caissons in clay for offshore wind turbine foundations." *Géotechnique*, 55(4), 287-296.

Karstunen, M., Krenn, H., Wheeler, S., Koskinen, M., and Zentar, R. (2005). "Effect of anisotropy and destructuration on the behavior of Murro Test embankment." *International Journal of Geomechanics*, 5(2), 87-97.

Karstunen, M., Wiltafsky, C., Krenn, H., Scharinger, F., and Schweiger, H. F. (2006). "Modelling the behaviour of an embankment on soft clay with different constitutive models." *International Journal for Numerical and Analytical Methods in Geomechanics*, 30(10), 953-982.

karstunen, M., and Yin, Z.-Y. (2010). "Modelling time-dependent behaviour of Murro test embankment." *Géotechnique*, 60(10), 735-749.

Kavvadas, M. (1982). "Non-linear consolidation around driven piles in clays." PhD, Massachusetts Institute of Technology.

Kim, D. (2004). "Comparisons of constitutive models for anisotropic soils." *KSCE J Civ Eng*, 8(4), 403-409.

Konrad, J.-M., and Roy, M. (1987). "Bearing capacity of friction piles in marine clay." *Géotechnique*, 37(2), 163-175.

Koskinen, M., Karstunen, M., and Wheeler, S. "Modelling destructuration and anisotropy of a soft natural clay." *Proc., Proceedings of the Fifth European Conference on Numerical Methods in Geotechnical Engineering*, Presses de l'ENPC, 11-20.

Lehane, B. M., and Jardine, R. J. (1994). "Displacement-pile behaviour in a soft marine clay." *Canadian Geotechnical Journal*, 31(2), 181-191.

Leoni, M., Karstunen, M., and Vermeer, P. A. (2008). "Anisotropic creep model for soft soils." *Géotechnique*, 58(3), 215-226.

Liyanapathirana, D. (2008). "A numerical model for predicting pile setup in clay." *Proceedings of GeoCongress 2008: Characterization, Monitoring, and Modeling of GeoSystems*, American Society of Civil Engineers, USA, 710-717.

McGinty, K. (2006). "The stress-strain behaviour of Bothkennar clay." PhD, University of Glasgow.

Niarchos, D. G. (2012). "Analysis of consolidation around driven piles in overconsolidated clay." MSc, Massachusetts Institute of Technology.

Nishimura, S., Minh, N. A., and Jardine, R. J. (2007). "Shear strength anisotropy of natural London Clay." *Géotechnique*, 57(1), 49-62.

O'Neill, M. W., Hawkins, R. A., and Audibert, J. M. (1982). "Installation of pile group in overconsolidated clay." *Journal of the Geotechnical Engineering Division*, 108(11), 1369-1386.

Pestana, J., Hunt, C., and Bray, J. (2002). "Soil deformation and excess pore pressure field around a closed-ended pile." *Journal of Geotechnical and Geoenvironmental Engineering*, 128(1), 1-12.

Randolph, M. F. (2003). "Science and empiricism in pile foundation design." *Géotechnique*, 53(10), 847-875.

Randolph, M. F., Carter, J. P., and Wroth, C. P. (1979). "Driven piles in clay: the effects of installation and subsequent consolidation." *Géotechnique*, 29(4), 361-393.

Roscoe, K. H., and Burland, J. (1968). "On the generalized stress-strain behaviour of wet clay." *Engineering Plasticity* 553-609.

Roy, M., Blanchet, R., Tavenas, F., and Rochelle, P. L. (1981). "Behaviour of a sensitive clay during pile driving." *Canadian Geotechnical Journal*, 18(1), 67-85.

Sekiguchi, H., and Ohta, H. (1977). "Induced anisotoropy and time dependency in clay." *9th ICSMFE, Tokyo, Constitutive Equations of Soils*, 17, 229-238.

Serridge, C. J., and Sarsby, R. W. (2008). "A review of field trials investigating the performance of partial depth vibro stone columns in a deep soft clay deposit." *Geotechnics of Soft Soils: Focus on Ground Improvement*, Taylor & Francis, 293-298.

Sivasithamparam, N. (2012). "Development and implementation of advanced soft soil models in finite elements." PhD, University of Strathclyde.

Sivasithamparam, N., Karstunen, M., and Bonnier, P. (2015). "Modelling creep behaviour of anisotropic soft soils." *Computers and Geotechnics*, 69, 46-57.

Soderberg, L. O. (1962). "Consolidation theory applied to foundation pile time effects." *Géotechnique*, 12(3), 217-225.

Svinkin, M. R., Morgano, C. M., and Morvant, M. "Pile capacity as a function of time in clayey and sandy soils." *Proc., Proceedings of the 5th International Conference and Exhibition on Piling and Deep Foundations*, Paper 1.11, pp.11-18.

Wheeler, S., Karstunen, M., and Naatanen, A. "Anisotropic hardening model for normally consolidated soft, clays." *Proc., 7th International Symposium on Numerical Models in Geomechanics (NUMOG VII)*, 33-40.

Wheeler, S. J., Näätänen, A., Karstunen, M., and Lojander, M. (2003). "An anisotropic elastoplastic model for soft clays." *Canadian Geotechnical Journal*, 40(2), 403-418.

Whittle, A., and Kavvadas, M. (1994). "Formulation of MIT-E3 Constitutive Model for Overconsolidated Clays." *Journal of Geotechnical Engineering*, 120(1), 173-198.

Xu, X. T., Liu, H. L., and Lehane, B. M. (2006). "Pipe pile installation effects in soft clay." *Proceedings of the Institution of Civil Engineers - Geotechnical Engineering*, 159(4), 285-296.

Yildiz, A. (2009). "Numerical modeling of vertical drains with advanced constitutive models." *Computers and Geotechnics*, 36(6), 1072-1083.

Yu, H.-S. (1990). "Cavity expansion theory and its application to the analysis of pressuremeters." PhD, University of Oxford.

Yu, H.-S. (2000). *Cavity expansion methods in geomechanics*, Springer.

Zwanenburg, C. (2013). "Application of SClay1 model to peat mechanics." Internal Report, Deltares, The Netherlands.

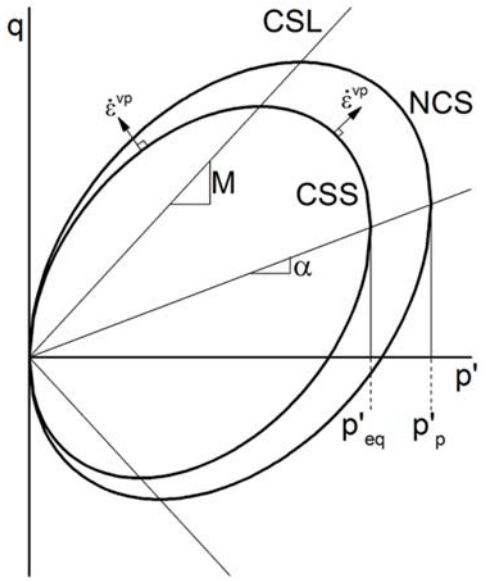

Fig. 1. Current State Surface (CSS) and Normal Consolidation Surfaces (NCS) of the Creep-SCLAY1 model and the direction of viscoplastic strains (triaxial stress space).

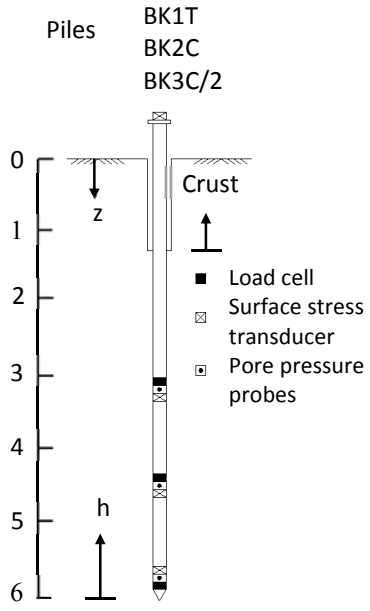

Fig. 2. Configuration of the piles.

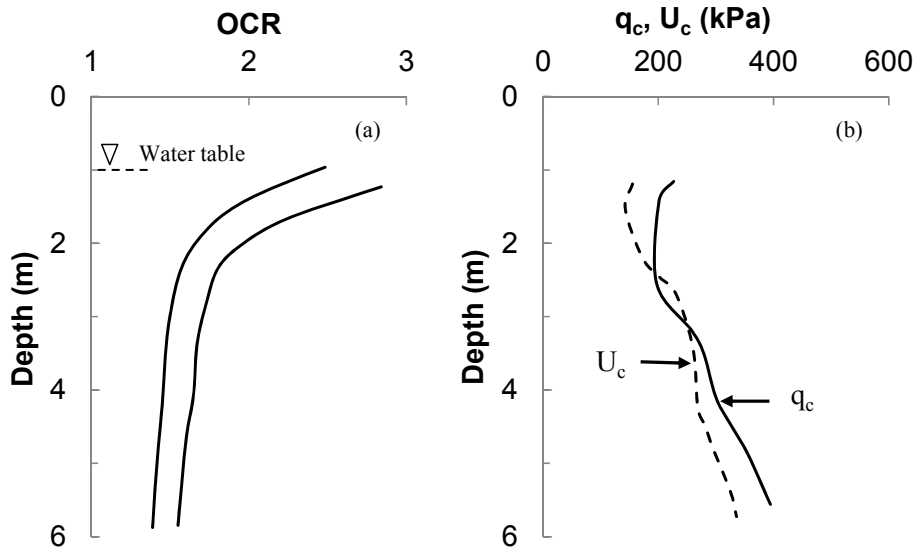

Fig. 3. Variations of a) OCR with depth obtained from oedometer tests, and b) end resistance (q_c) and pore pressure (U_c) with depth obtained from *in-situ* piezocone tests [data from Lehane and Jardine (1994)].

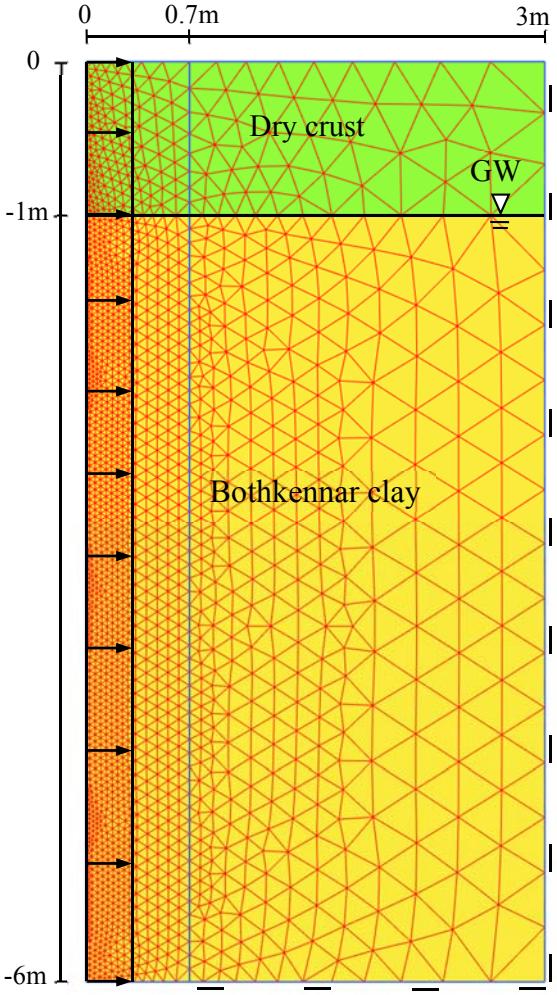

Fig. 4. Geometry of the boundary value problem and the idealised soil profile.

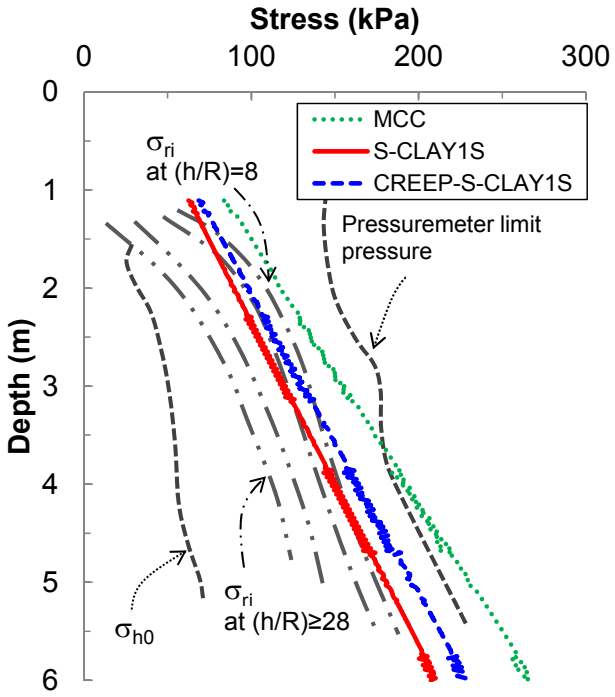

Fig. 5. Comparison between measured and predicted radial total stresses at the pile surface, after pile installation [data from Lehane and Jardine (1994)].

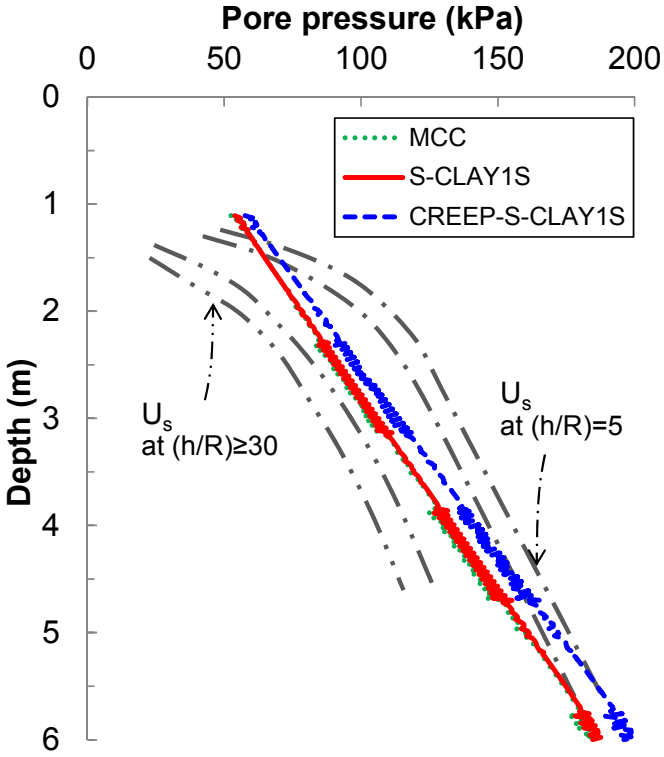

Fig. 6. Comparison between measured and predicted pore pressures at the pile surface, after pile installation [data from Lehane and Jardine (1994)].

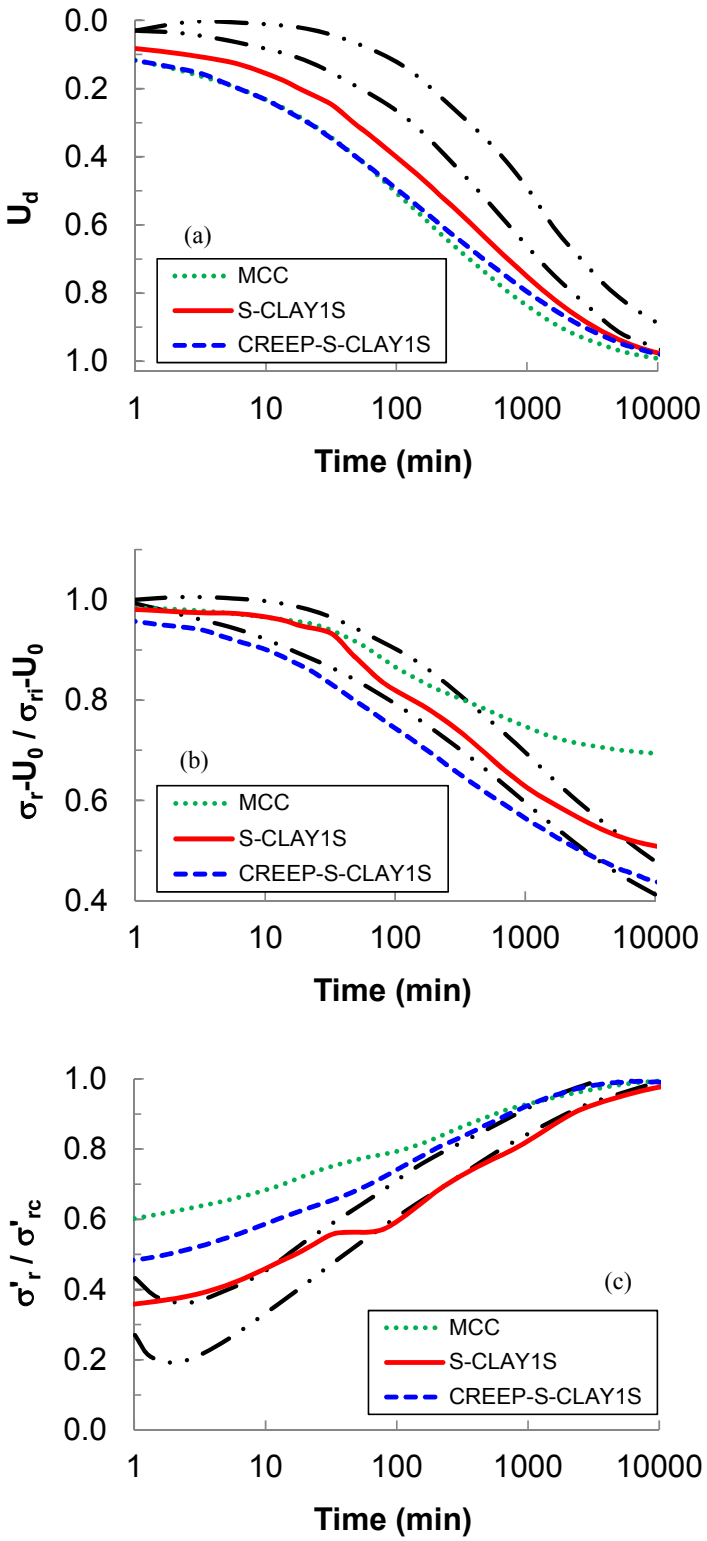

Fig. 7. Comparison between simulation results with measurements during equalisation for a) pore pressure; b) radial total stress; c) radial effective stress [data from Lehane and Jardine (1994)].

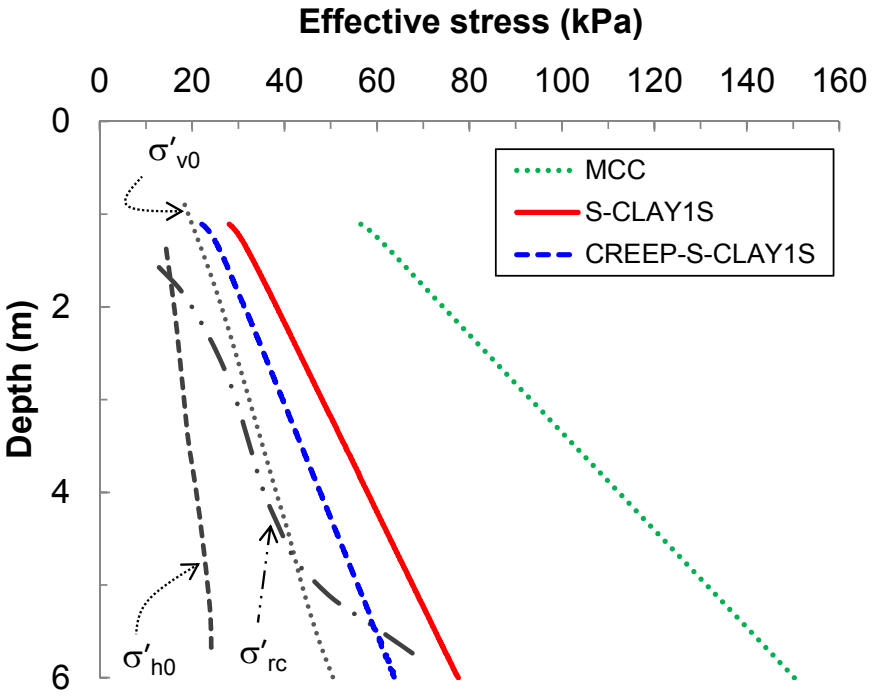

Fig. 8. Comparison between measured and predicted radial effective stresses on the pile surface at depth (h/R) = 28, after equalisation [data from Lehane and Jardine (1994)].

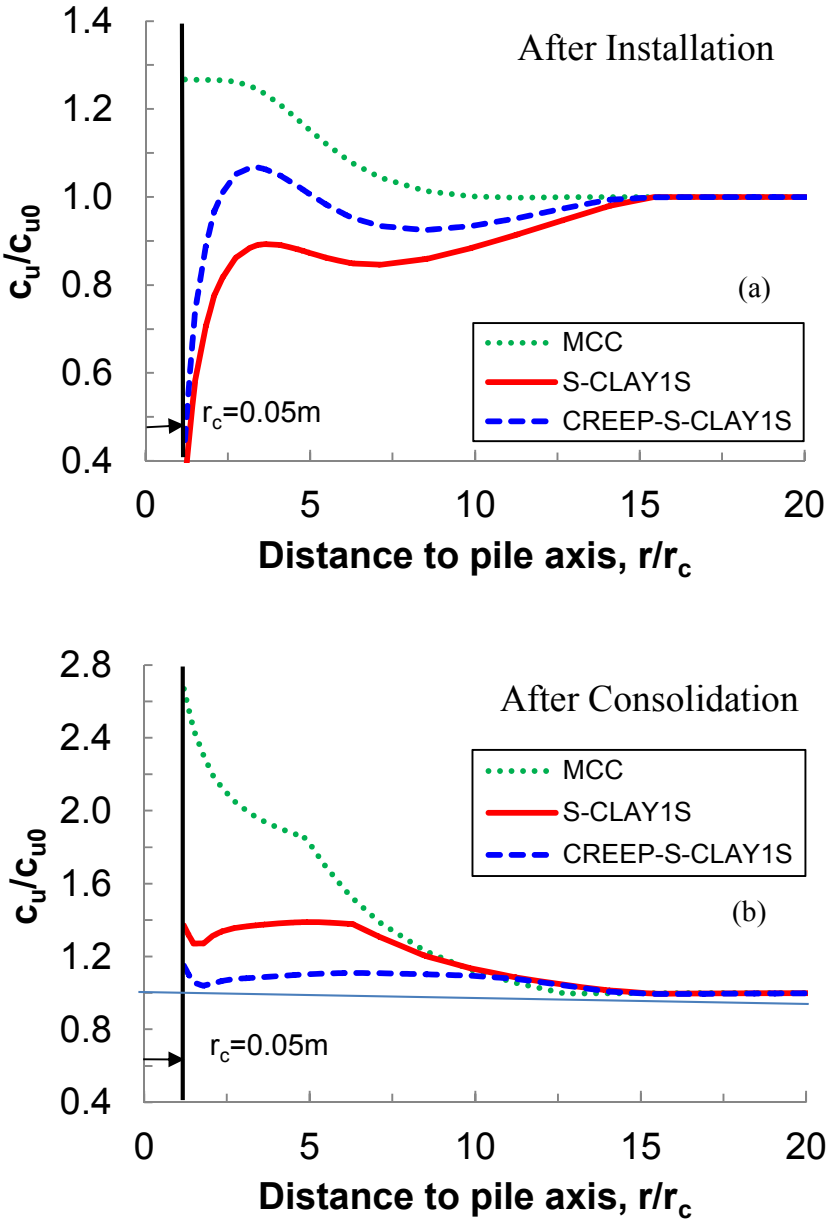

Fig. 9 Simulation results for relative variations of undrained shear strength due to pile driving, a) after installation, b) after equalisation.

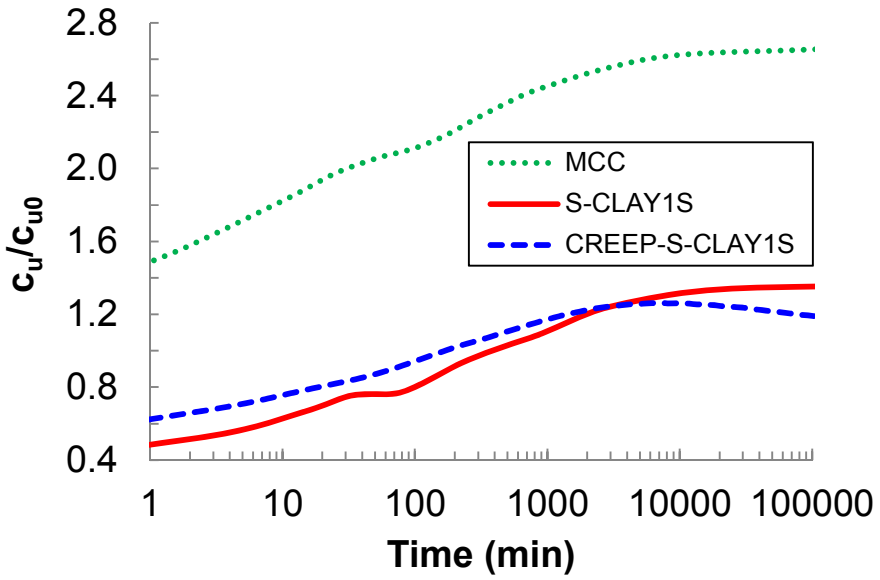

Fig. 10 Simulation results for relative variations of undrained shear strength with time.

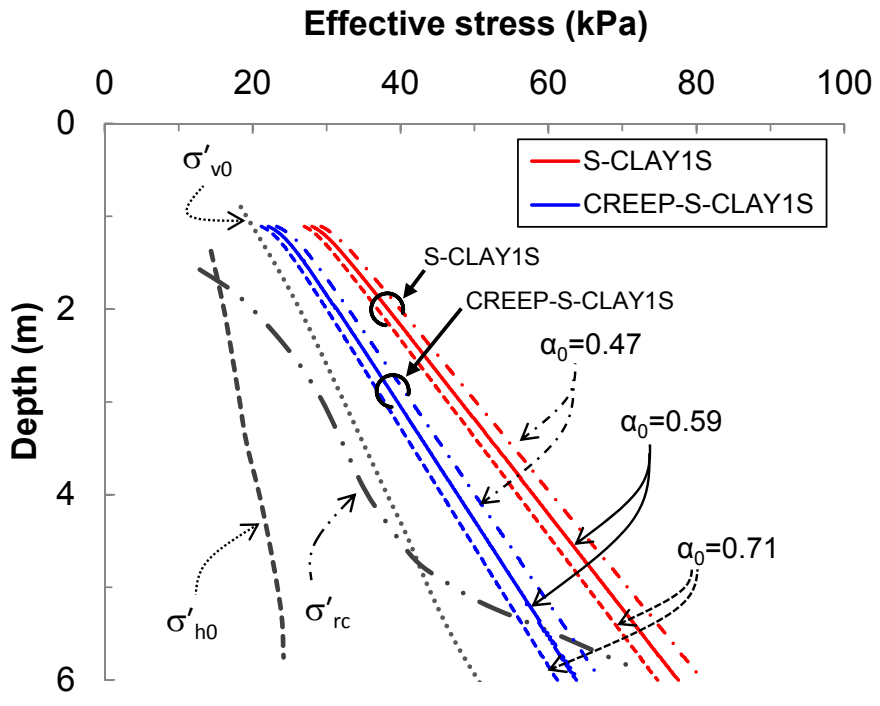

Fig. 11. Effect of anisotropy parameter alterations on radial effective stress predictions (at pile surface at depth (h/R) = 28, after equalisation) [data from Lehane and Jardine (1994)].

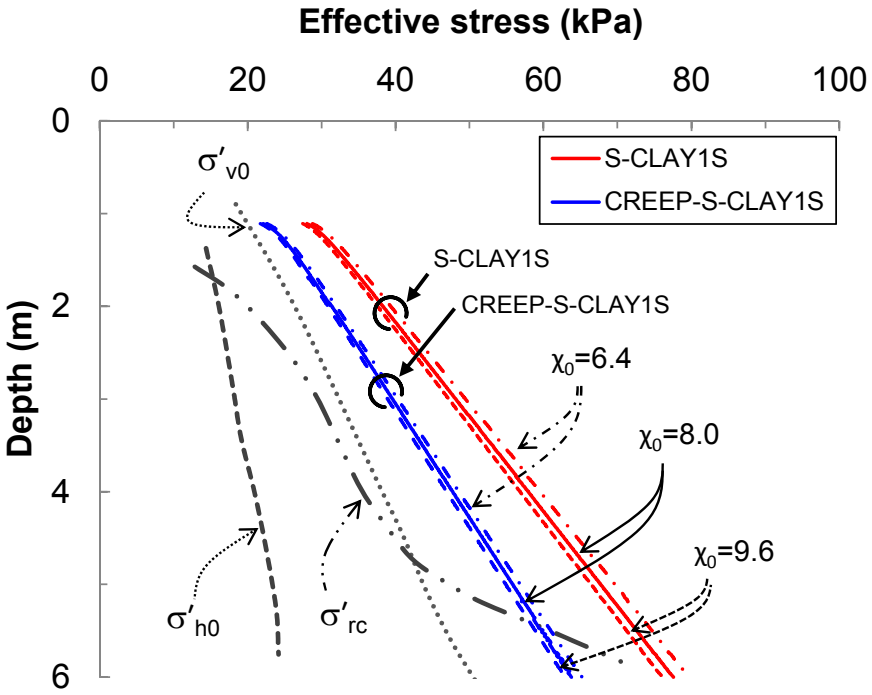

Fig. 12. Effect of destructuration parameter alterations on radial effective stress predictions (at pile surface at depth (h/R) = 28, after equalisation) [data from Lehane and Jardine (1994)].

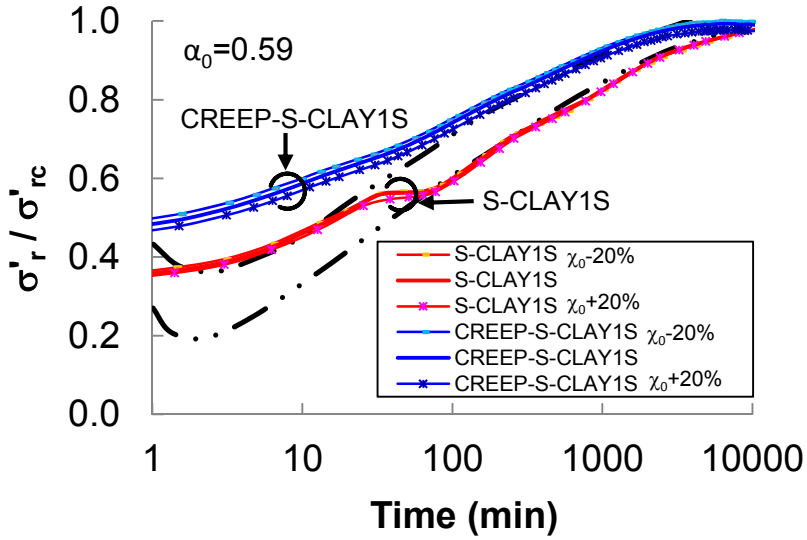

Fig. 13. Effect of anisotropy parameter alterations on variations of radial effective stress during equalisation [data from Lehane and Jardine (1994)].

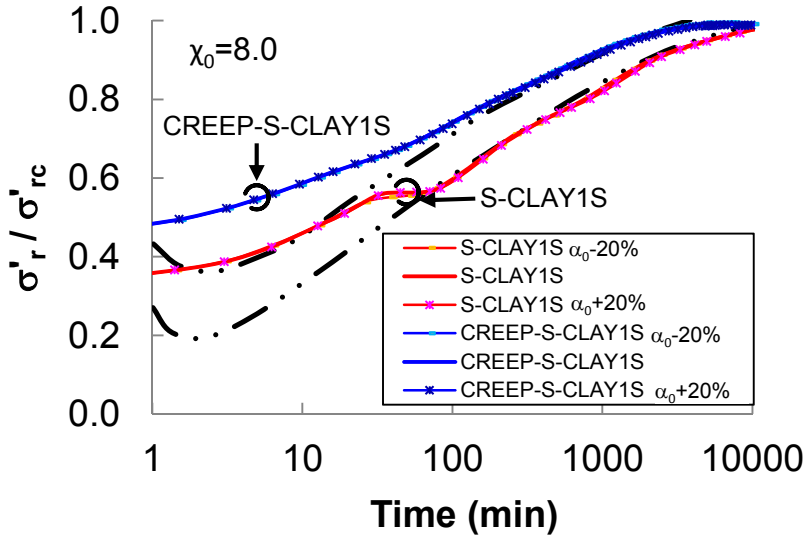

Fig. 14. Effect of destructuration parameter alterations on variations of radial effective stress during equalisation [data from Lehane and Jardine (1994)].

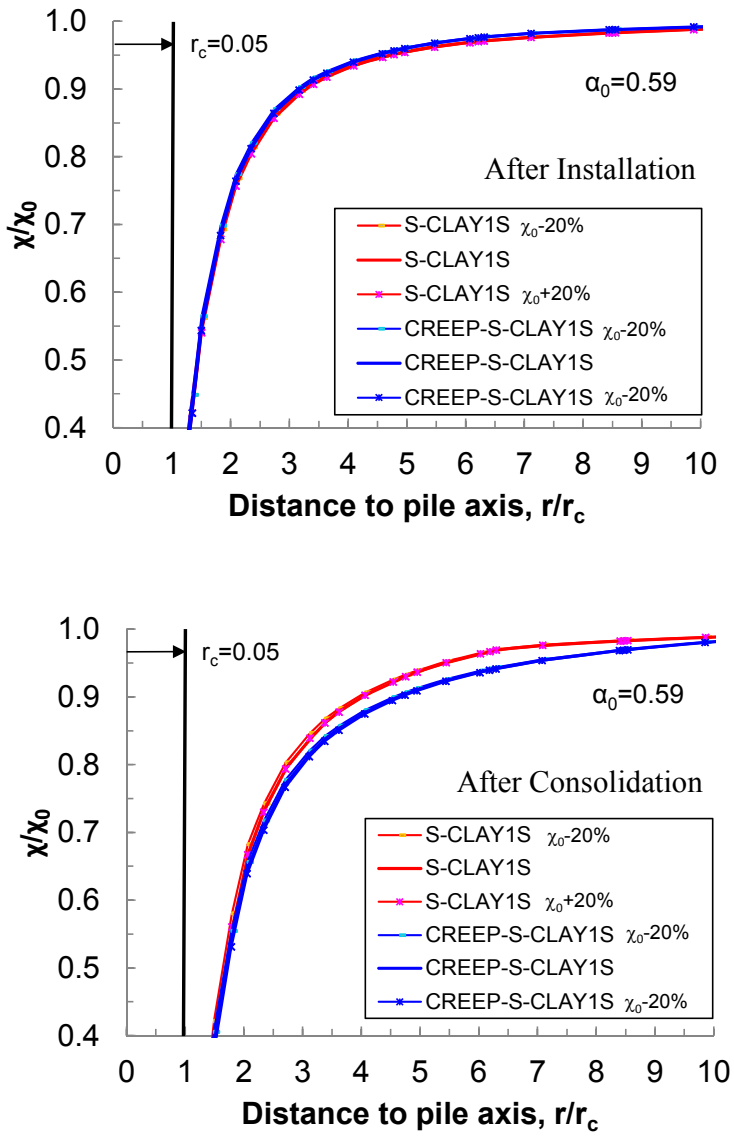

Fig. 15 Simulation results for relative variations of destructuration parameter due to pile driving.

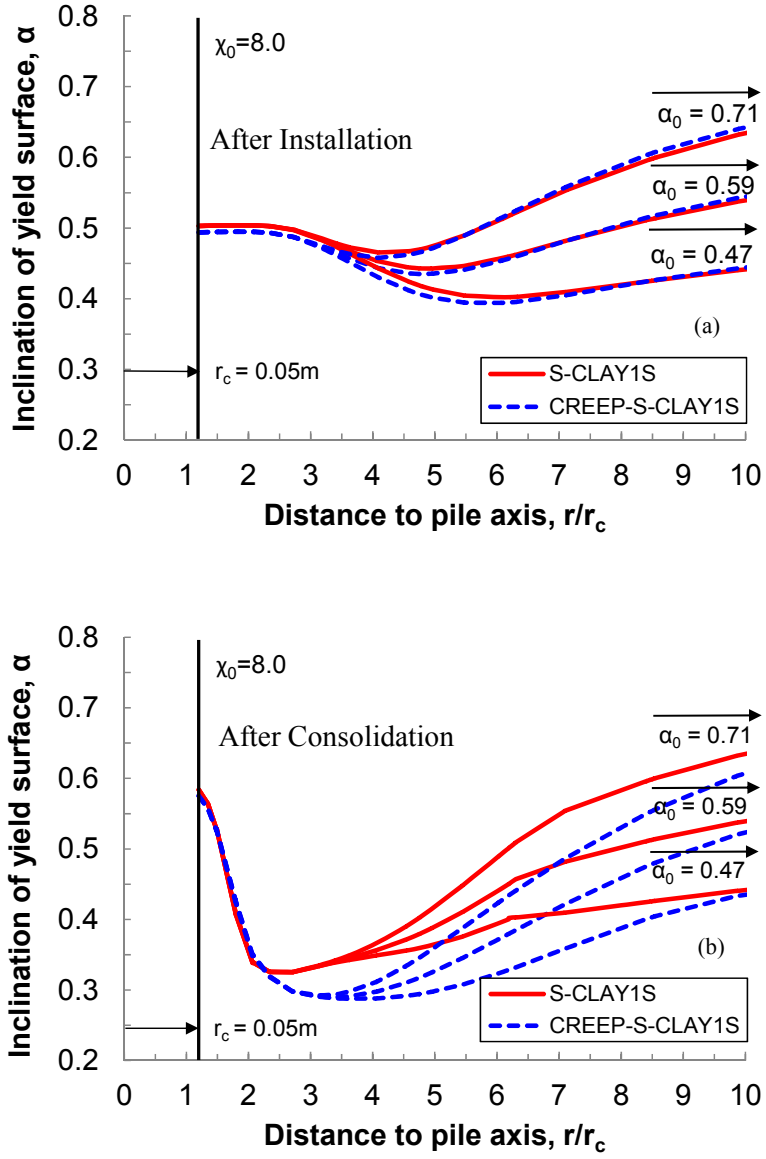

Fig. 16 Simulation results for relative variations of α_0 due to pile driving.

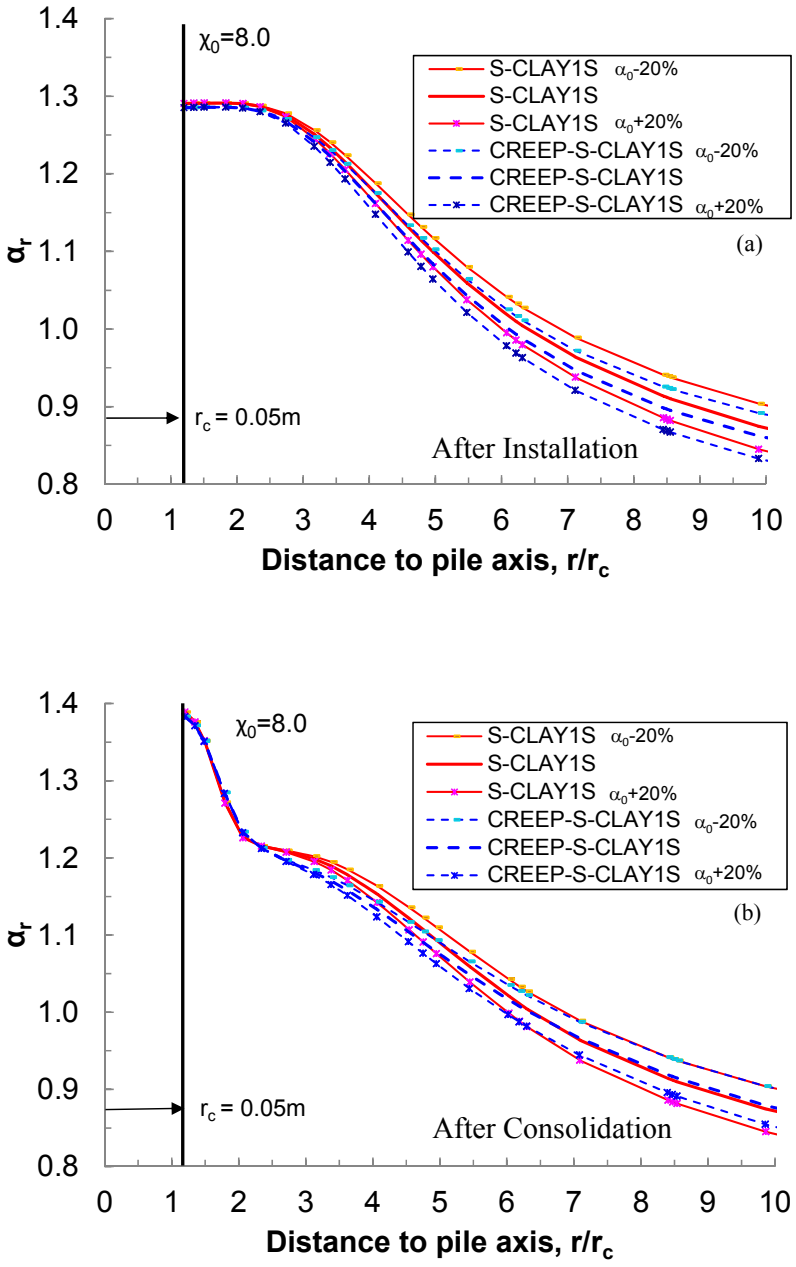

Fig. 17 Changes of α_r due to pile driving with different initial anisotropy values.

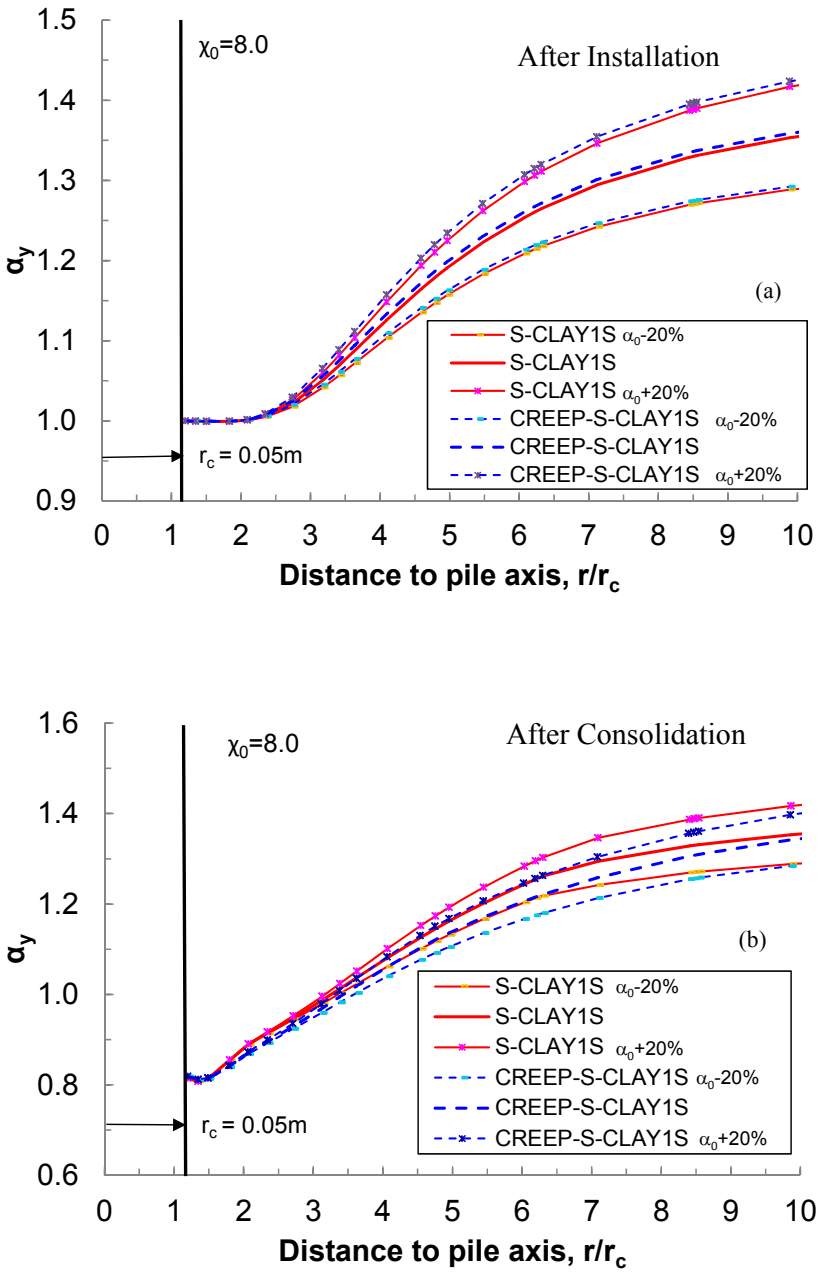

Fig. 18 Changes of α_y due to pile driving with different initial anisotropy values.

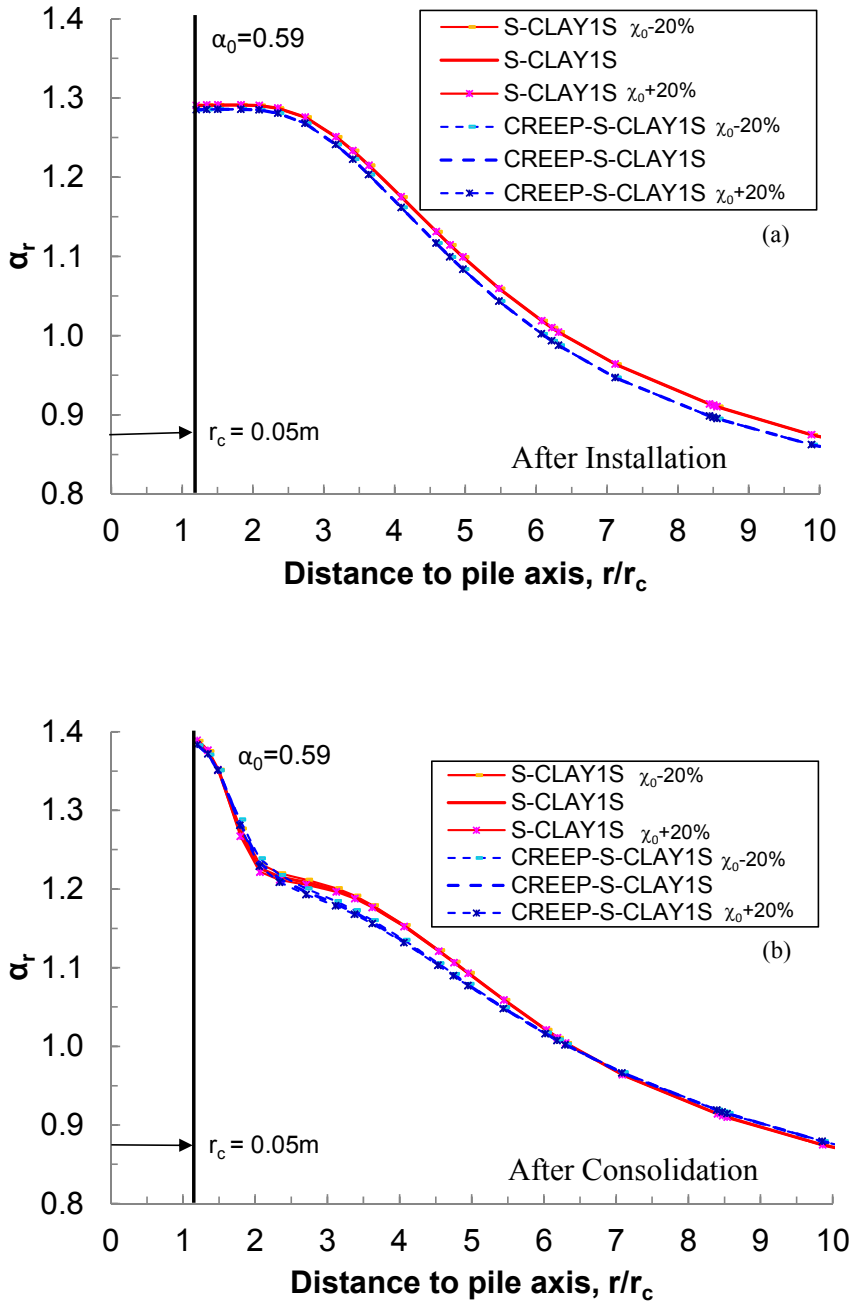

Fig. 19 Changes of α_r due to pile driving with different initial bonding values.

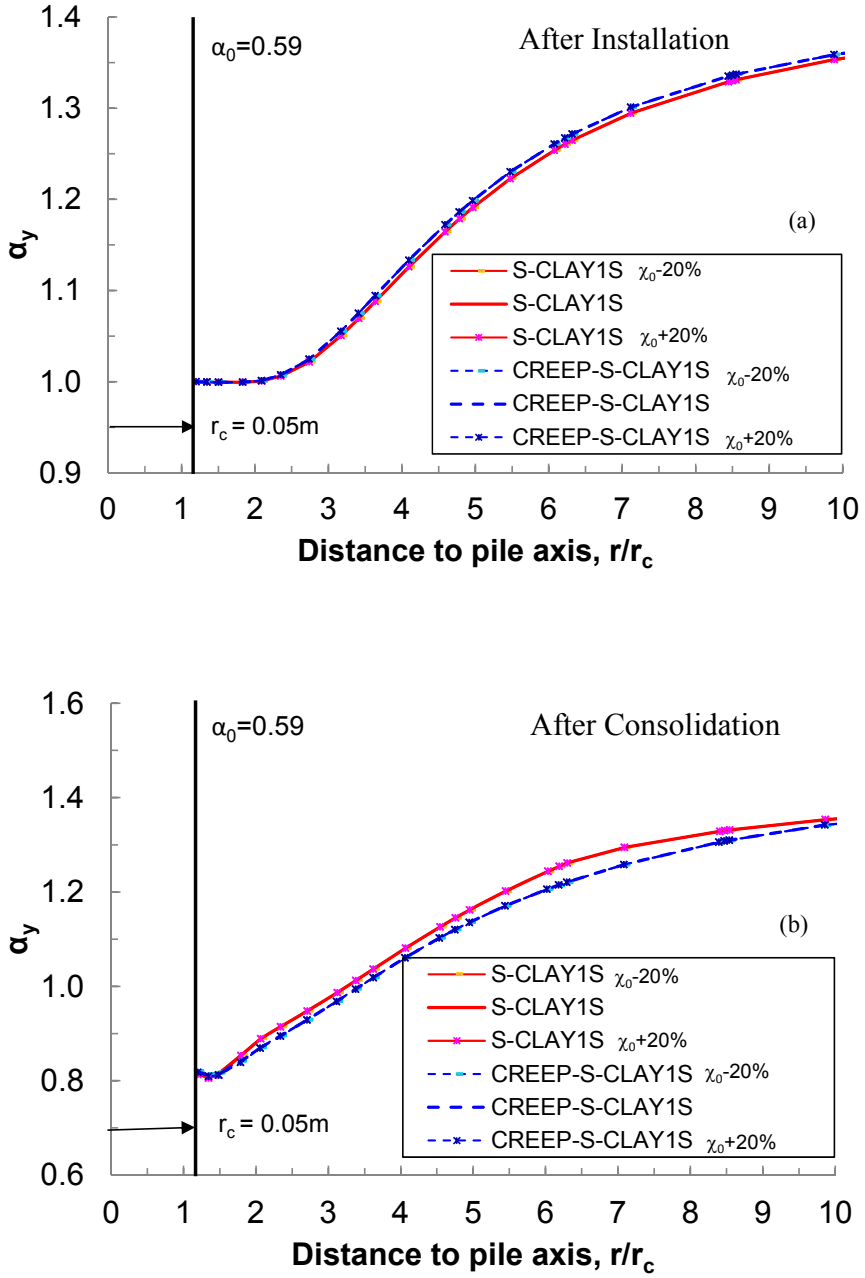

Fig. 20 Changes of α_y due to pile driving with different initial bonding values.